Molecular Microbiology (2008) 70(5), 1166–1179 ■
doi:10.1111/j.1365-2958.2008.06469.x
First published online 20 October 2008

MinJ (YvjD) is a topological determinant of cell division in *Bacillus subtilis*

Joyce E. Patrick and Daniel B. Kearns*
Department of Biology, Indiana University, 1001 East Third Street, Bloomington, IN 47405, USA.

Summary

In *Bacillus subtilis*, FtsZ ring formation and cell division is favoured at the midcell because the inhibitor proteins MinC and MinD are indirectly restricted to the cell poles by the protein DivIVA. Here we identify MinJ, a topological determinant of medial FtsZ positioning that acts as an intermediary between DivIVA and MinD. Due to unrestricted MinD activity, cells mutated for *minJ* exhibited pleiotropic defects in homologous recombination, swarming motility and cell division. MinJ restricted MinD activity by localizing MinD to the cell poles through direct protein–protein interaction. MinJ itself localized to cell poles in a manner that was dependent on DivIVA. MinJ is conserved in other low G+C Gram-positive bacteria and may be an important component of cell division site selection in these organisms.

Introduction

During growth, bacteria elongate and then divide into two identical daughter cells by a process called binary fission. Binary fission is initiated by FtsZ, a homologue of eukaryotic tubulin that polymerizes into a ring at the cytoplasmic surface of the cell membrane and recruits the cell wall biosynthesis machinery (Bi and Lutkenhaus, 1991; Erickson, 1995; Errington *et al*., 2003; Pichoff and Lutkenhaus, 2005). FtsZ is a GTPase for which GTP binding promotes polymerization, and GTP hydrolysis promotes depolymerization, membrane constriction and ultimately septation (de Boer *et al*., 1992; Mukherjee and Lutkenhaus, 1994; 1998; Stricker *et al*., 2002; Osawa *et al*., 2008). Bacteria divide symmetrically because a ring of FtsZ is directed to form at the precise middle of the cell and the fidelity of FtsZ positioning is governed by a separate set of proteins that constitute the 'Min' system (de Boer *et al*., 1989).

Accepted 15 September, 2008. *For correspondence. E-mail dbkearns@indiana.edu; Tel. (+1) 812 856 2523; Fax (+1) 812 855 6705.

The core of the Min system is two highly conserved proteins MinC and MinD that cooperate to inhibit FtsZ ring formation (de Boer *et al*., 1989; Levin *et al*., 1992; Varley and Stewart, 1992). MinC directly interacts with FtsZ to destabilize the FtsZ ring (Hu *et al*., 1999; Dajkovic *et al*., 2008). MinD is a membrane-associated ATPase that recruits MinC to the membrane and is necessary for MinC activity (Hu *et al*., 2002; Johnson *et al*., 2002). Thus, MinC and MinD coat the inside surface of the cytoplasmic membrane and prevent the initiation of cell division wherever they are found. A third component, called a topological determinant, is required to restrict MinC/MinD activity to the cell poles thereby allowing FtsZ to form rings at the midcell. Mutation of either *minC* or *minD* results in indiscriminate FtsZ polymerization and allows cell division to take place at polar sites that give rise to anucleate 'minicells' (Levin *et al*., 1998). In contrast, mutation of the topological determinant leads to unrestricted inhibition of cell division by MinC and MinD and cell filamentation (de Boer *et al*., 1989; Cha and Stewart, 1997; Edwards and Errington, 1997).

In the Gram-negative bacterium *Escherichia coli*, the topological determinant is a small soluble protein called MinE that dynamically antagonizes the MinC and MinD cell division inhibitors (Raskin and de Boer, 1997; Ma *et al*., 2004). First, MinC and MinD polymerize as a cytoplasmic shell that spreads from one cell pole towards the midcell. Next, MinE forms a ring and depolymerizes MinC and MinD back towards the pole of origin. Finally, a new shell of MinC and MinD forms at the opposite cell pole and the cycle repeats itself (Raskin and de Boer, 1999; Hale *et al*., 2001). The result of the dynamic antagonism is that a high local concentration of MinC and MinD oscillates from one pole to the other. Oscillations happen rapidly, so that on average, the lowest concentration of MinC and MinD is found at the midcell where FtsZ preferentially polymerizes to initiate cell division (Meinhardt and de Boer, 2001).

In the Gram-positive bacterium *Bacillus subtilis*, the topological determinant is thought to be the tropomyosin-like coiled-coil protein DivIVA that antagonizes MinC and MinD by statically restricting their subcellular localization (Cha and Stewart, 1997; Edwards and Errington, 1997; Edwards *et al*., 2000). According to the 'polar-piloting' model, DivIVA localizes to both cell poles and tethers the

shells of MinC and MinD. As growing cells get longer, a gap forms at midcell that is depleted for the inhibitors and allows for the medial formation of the FtsZ ring (Marston *et al*., 1998; Marston and Errington, 1999). Thus, although MinC and MinD do not oscillate in *B. subtilis*, their activity is nonetheless restricted to the poles by DivIVA. What controls DivIVA localization is unknown but DivIVA localizes at an early step during the formation of the nascent septum and recruits MinC and MinD to prevent the reinitiation of cytokinesis (Edwards *et al*., 2000; Hamoen and Errington, 2003; Harry and Lewis, 2003). No direct interaction between DivIVA and either MinC or MinD has been reported raising the possibility that other proteins may participate in the polar-piloting model.

In this work, we serendipitously discovered a new topological determinant of the *B. subtilis* Min system. While studying the *yvjD* gene reportedly involved in a multicellular behaviour called swarming motility (Kearns and Losick, 2003; Calvio *et al*., 2005), it became apparent that the *yvjD* mutant had pleiotropic effects, the most dramatic of which was a defect in cell division. Here we change the name of YvjD to MinJ because MinJ antagonized the cell division inhibitors MinC and MinD, and MinJ localized to the sites of septum formation in a DivIVA-dependent manner.

Results

minJ *(yvjD) is transcribed independently from* swrA

The *B. subtilis swrA* gene encodes SwrA, a protein that activates flagellar gene expression and is required for a rapid, social form of surface motility called swarming (Kearns *et al*., 2004; Calvio *et al*., 2005; Kearns and Losick, 2005). Recently it has been reported that *swrA* (*swrAA*) is co-transcribed with the adjacent gene *yvjD* (*swrAB*), and that the products of both genes interact to regulate motility (Fig. 1A, Calvio *et al*., 2005). To test the hypothesis that the two genes form an operon, transcriptional reporters were generated by separately cloning the regions immediately upstream of *swrA* (P_{swrA}) and *yvjD* (P_{minJ}) in front of a promoter-less copy of the *lacZ* gene encoding β-galactosidase and were integrated at an ectopic locus in the chromosome. Both reporters produced β-galactosidase activity that was significantly greater than the promoter-less *lacZ* that served as a negative control (Fig. 1B). Thus, *yvjD* was transcribed from a promoter that was separate from the promoter of *swrA*.

To explore YvjD function, we generated an in-frame marker-less deletion of the *yvjD* gene in an undomesticated strain of *B. subtilis*. During the course of our investigation, we found that the *yvjD* mutant was highly pleiotropic. We changed the name of YvjD to MinJ because it was required for homologous recombination, wild-type swarming behaviour and, most significantly, cell division (see below).

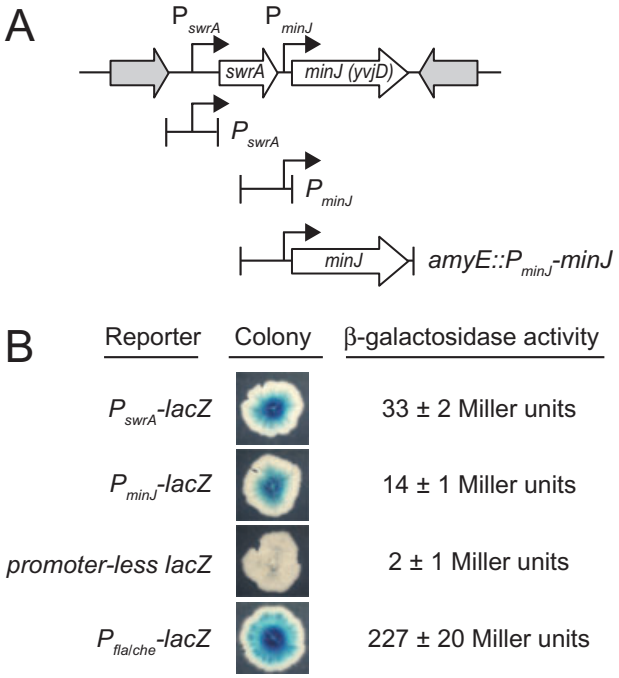

Fig. 1. The *minJ* genetic region.
A. Open arrows indicate open reading frames. Bent arrows indicate the location of promoters. 'P_{swrA}' and 'P_{minJ}' indicate the boundaries of the indicated promoters used in the β-galactosidase assay in (B). '*amyE::*P_{minJ}*-minJ*' indicates the boundaries of the *minJ* complementation construct.
B. Transcriptional reporters were generated in which the gene encoding β-galactosidase (*lacZ*) was fused to the promoter region of *swrA* (P_{swrA}) or *minJ* (P_{minJ}) and introduced at an ectopic site of an otherwise wild-type strain (DS796 and DS1576 respectively). Strains containing a promoter-less *lacZ* gene (DS4291) and a *lacZ* gene expressed under the control of the $P_{fla/che}$ promoter (DS791) were included as negative and positive controls respectively. Colonies grown in the presence of 100 μg ml^{-1} of the chromogenic β-galactosidase substrate X-Gal are shown. β-Galactosidase-specific activity was measured from mid-log-phase liquid grown cells and presented in Miller units as the average and standard deviation of three replicates.

MinJ is required for homologous recombination

We immediately encountered difficulties with the genetic manipulation of the chromosome of *minJ* strains. SPP1 phage-mediated transduction of either chloramphenicol or kanamycin resistance cassettes integrated at the ectopic *amyE* or *lacA* loci, respectively, resulted in tens to hundreds of transductants when wild-type cells were used as the recipient but no transductants were obtained when the *minJ* mutant was used as the recipient (Table 1). Similarly, no transductants were obtained when *minJ* was the recipient and a variety of other antibiotic resistance cassettes integrated at various other loci in the chromosome were

Table 1. *minJ* is defective in homologous recombination.

Recipient		Donor *amyE::cat*	Donor *lacA::kan*	Donor pMarA *kan*	Donor *amyE::P$_{minJ}$-minJ cat*
Wild type	(6.6×10^8)	219	30	756	192
Δ*minJ*	(1.4×10^8)	0	0	183	68
Δ*minJ amyE::P$_{minJ}$-minJ*	(9.8×10^8)	N/A	51	972	N/A
Δ*minJ minD*	(7.3×10^8)	111	N/A	N/A	172
minD	(9.6×10^8)	217	N/A	N/A	183
divIVA	(1.4×10^8)	0	0	34	0

Numbers in table indicate the number of colonies resulting from a genetic cross mediated by SPP1 generalized transduction between the indicated donor strain (columns) and the indicated recipient strain (rows). The number in parentheses is the number of recipient cells used in each cross. N/A indicates 'not applicable' due to an incompatibility of the donor allele antibiotic resistance cassette with an antibiotic resistance cassette present in the parental background. The strains used as recipients in this table are as follows: 3610, DS2845, DS2945, DS3186, DS3774 and DS4146.

used as donors (data not shown). In contrast, hundreds of colonies were obtained when an extra-chromosomally maintained plasmid was delivered to either the wild type or the *minJ* mutant by generalized transduction (pMarA, Table 1). We conclude that *minJ* was neither resistant to the transducing phage nor recalcitrant to DNA uptake. Rather, *minJ* appeared to have a defect in homologous recombination.

Cells defective in homologous recombination exhibit an increase in sensitivity to DNA damage by UV radiation (Howard-Flanders *et al*., 1969; Munakata, 1974). Wild-type *B. subtilis* suffered a two-log decrease in viable cells after 1 min of exposure to UV light (Fig. S1). In contrast, the *minJ* mutant suffered a four-log decrease in viable cells from the same exposure. The inability of *minJ* to incorporate donor DNA and an increased sensitivity to UV radiation are both consistent with a defect in homologous recombination.

The *minJ* homologous recombination defect could be complemented *in trans*. DNA was efficiently recombined into the *minJ* mutant chromosome only when the donor DNA contained a complementing fragment that included the *minJ* gene and the promoter of *minJ* (P_{minJ}) (Table 1). Once integrated, the complementation construct rescued the ability of the *minJ* mutant to serve as a recipient in all generalized transduction experiments tested (Table 1, data not shown). To circumvent the genetic challenges associated with the reduced recombination in the *minJ* background, all genetic constructs involving *minJ* were first generated in a strain containing the complementation construct at the ectopic locus. In a second step, the complementation construct was eliminated by replacement with an antibiotic resistance cassette.

MinJ is required for wild-type swarming behaviour

MinJ has been reported to regulate motility in laboratory strains (Calvio *et al*., 2005). Unlike laboratory strains, undomesticated strains of *B. subtilis* have a robust form of surface motility called swarming, and to evaluate the role of MinJ in motility, the *minJ* mutant was tested for swarming behaviour (Kearns and Losick, 2003). Swarming wild-type cells spread rapidly as a monolayer and completely colonized the surface of a swarm agar plate (wild type, Fig. 2, Movie S1). In contrast, the surface movements of the *minJ* mutant were strikingly unusual and manifested as spiralling whorls on the surface of the media (Δ*minJ*, Fig. 2, Movie S2). The unusual behaviour was the direct consequence of the absence of *minJ* as behaviour indis-

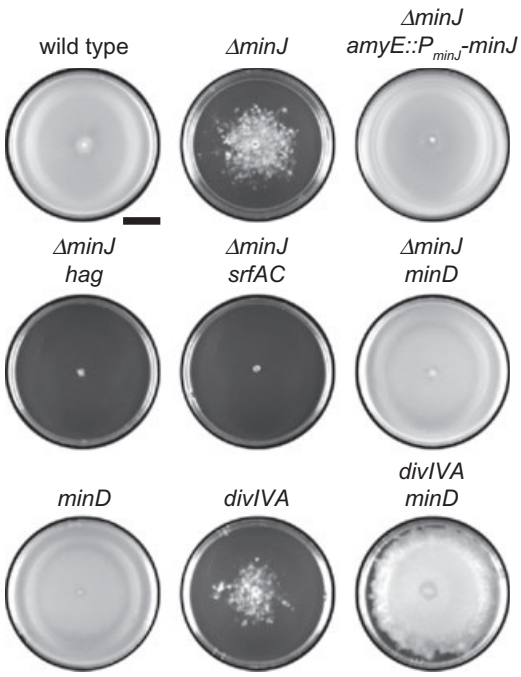

Fig. 2. Cells mutated for *minJ* exhibit aberrant swarming behaviour. Circles are top views of swarm agar Petri plates. Plates were inoculated with wild type (3610), Δ*minJ* (DS2845), Δ*minJ* (*amyE::P$_{minJ}$-minJ*) (DS2945), Δ*minJ hag* (DS3277), Δ*minJ srfAC* (DS3406), Δ*minJ minD* (DS3186), *minD* (DS3774), *divIVA* (DS4146), *divIVA minD* (DS4151) and filmed against a black background such that zones of bacterial colonization appear white and uncolonized agar appears black. Incomplete colonization of the surface is indicative of a swarming motility defect. Scale bar is 2 cm.

tinguishable from wild type was restored when a *minJ* complementation construct was introduced at the *amyE* locus (Δ*minJ amyE::*P_{minJ}*-minJ*, Fig. 2).

Swarming motility is powered by flagellar rotation and requires the secretion of a surfactant (Kearns and Losick, 2003; Kearns *et al*., 2004). To determine whether the unusual behaviour of *minJ* was a manifestation of swarming motility, double mutants were generated that were simultaneously disrupted for both *minJ* and either flagellum assembly (*hag*) or surfactin biosynthesis (*srfAC*). Both double mutants showed a more severe defect in surface colonization than the *minJ* single mutant indicating that the behaviour of *minJ* was an impaired form of swarming motility (Fig. 2). We conclude that MinJ is not explicitly required for swarming but that the absence of MinJ alters swarming behaviour.

MinJ is required for efficient cell division

We noticed that cells of the *minJ* mutant appeared to be elongated compared with the wild type (Movies S1 and S2). Consistent with this observation, both wild type and the *minJ* mutant exhibited similar growth rates when grown in broth culture but the *minJ* mutant had fivefold fewer colony-forming units per OD_{600} (Fig. S2). The long cells and reduction in colony-forming units could have been either due to an inability of the cells to divide or due to a defect in cell separation following cell division; fluorescence microscopy of cell membranes and chromosomes was conducted to distinguish the two possibilities. Compared with the wild type, the *minJ* mutant grew as long filaments in which cell division septa were rare (Fig. 3A and B). The *minJ* mutant contained many evenly spaced and clearly segregated nucleoids indicating that there was no deficiency in chromosome replication or segregation. Complementation of *minJ* at an ectopic locus restored cell division to wild-type levels (Fig. 3C). We conclude that MinJ is not essential for growth but is nonetheless necessary for efficient cell division.

Cell division is initiated when the FtsZ protein polymerizes into a ring (Z-ring) at the nascent division site. To determine whether *minJ* was defective in Z-ring formation, we monitored the position of yellow fluorescent protein (YFP) fused to ZapA (*zapAΩYFP*), a protein that promotes FtsZ polymerization and colocalizes with FtsZ rings (Gueiros-Filho and Losick, 2002). In wild-type cells, ZapA–YFP formed intense, medial bands near the middle of each cell (Fig. 4A). In *minJ* mutants, however, ZapA–YFP localization was impaired, and ZapA formed irregular, weak foci (Fig. 4B). We infer that MinJ is required for

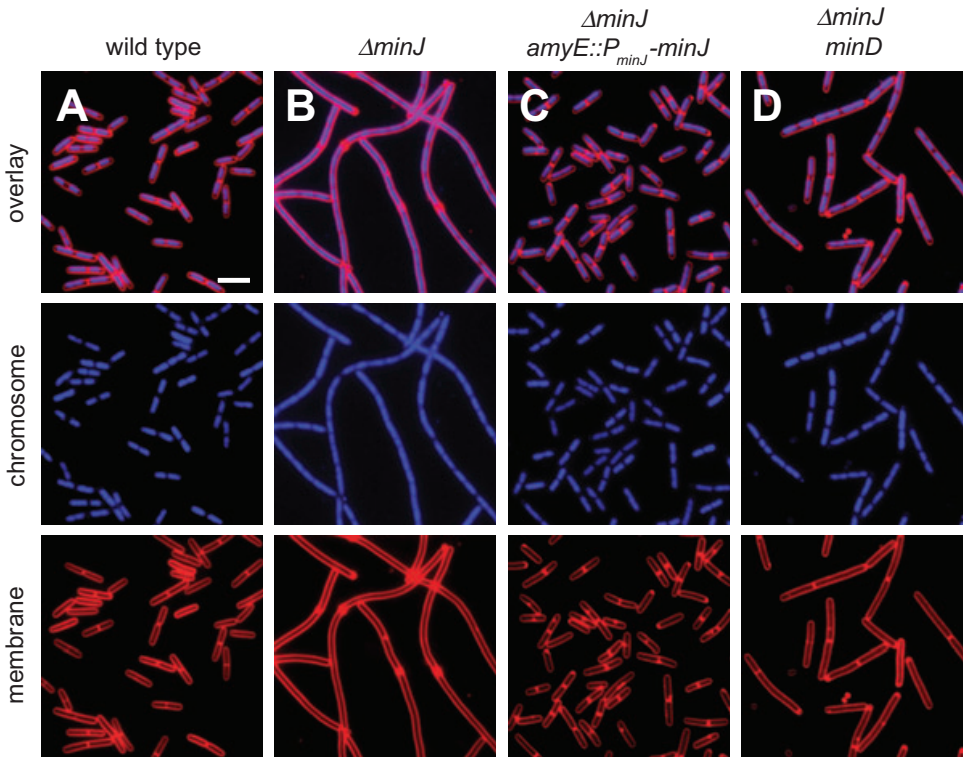

Fig. 3. Cells mutated for *minJ* are filamentous. Fluorescence microscopy of wild type (A, 3610), Δ*minJ* (B, DS2845), Δ*minJ* (*amyE::*P_{minJ}*-minJ*) (C, DS2945) and Δ*minJ minD* (D, DS3293) were grown to mid-exponential phase and stained with FM 4-64 (membrane, false coloured red) and DAPI (chromosome, false coloured blue). Scale bar is 4 μm.

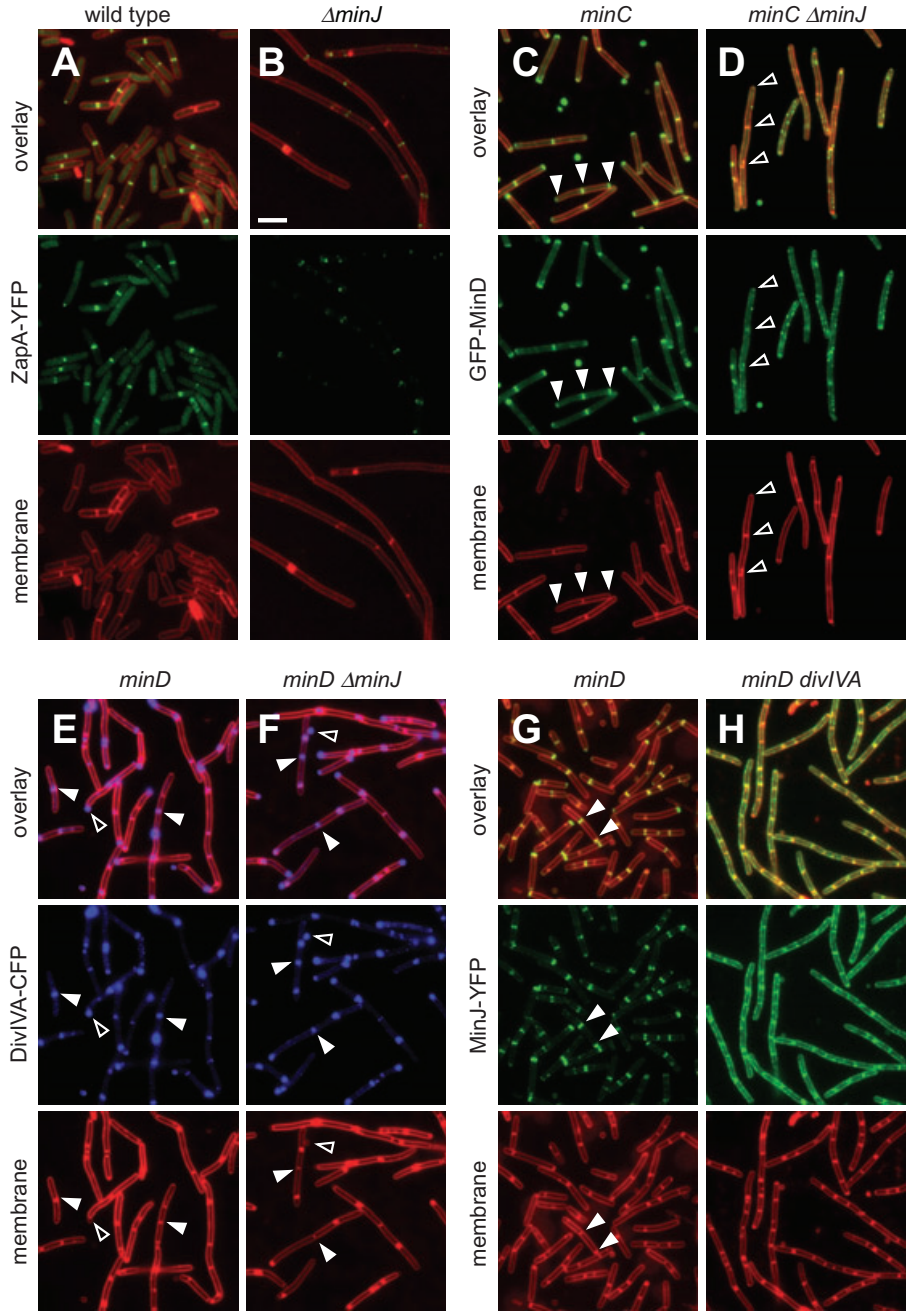

Fig. 4. MinJ localizes to cell poles in a DivIVA-dependent manner and MinJ is required for the proper localization of FtsZ and MinD.
A and B. Fluorescence microscopy of wild type (A, DS3621) and Δ*minJ* mutant (B, DS3799) cells expressing YFP fused to an FtsZ-associated protein (ZapA–YFP, false coloured green) that were grown to exponential phase and stained with FM 4-64 (membrane, false coloured red).
C and D. Fluorescence microscopy of *minC* single mutant (C, DS4322) and *minC* Δ*minJ* double mutant (D, DS4323) cells expressing GFP fused to MinD (GFP–MinD, false coloured green) grown to exponential phase and stained with FM 4-64 (membrane, false coloured red). Closed carets indicate septa and poles at which MinD is enriched. Open carets indicate septa and poles in which MinD is not enriched.
E and F. Fluorescence microscopy of *minD* single mutant (E, DS4155) and *minD minJ* double mutant (E, DS4153) cells expressing CFP fused to DivIVA (DivIVA–CFP, false coloured blue) that were grown to exponential phase and stained for FM 4-64 (membrane, false coloured red). Closed caret indicates a site of DivIVA septal localization. Open caret indicates a site of DivIVA minicell localization.
G and H. Fluorescence microscopy of *minD* single mutant (C, DS3840) and *minD divIVA* double mutant (D, DS4151) cells expressing YFP fused to MinJ (MinJ–YFP, false coloured green) that were grown to exponential phase and stained for FM 4-64 (membrane, false coloured red). Closed carets indicate sites of MinJ polar localization.
Scale bar is 4 μm.

efficient cell division because in the absence of MinJ, cells failed to form FtsZ rings like the wild type.

MinJ interacts with the 'Min' system

Cells mutated for *minJ* were highly pleiotropic and had defects in homologous recombination, swarming motility and cell division. To determine the genetic hierarchy of these defects, we selected for second-site mutations that would at least restore robust swarming motility to the *minJ* mutant. The *minJ* mutant was mutagenized with transposons and seven strains were independently isolated that had improved swarming motility. All seven isolates contained disruptions in either the *minC* or *minD* genes that encode inhibitors of FtsZ polymerization (Marston and Errington, 1999). In addition to exhibiting rescued swarming motility (Fig. 2), cells simultaneously mutated for *minD* and *minJ* were less filamentous (Fig. 3D), generated minicells (data not shown) and were improved for homologous recombination (Table 1). In each case, the phenotype of the *minD* (or *minC*) mutation was epistatic to that of the *minJ* mutation (data not shown). We conclude that the primary function of MinJ is to antagonize the MinC and MinD cell division inhibitors. Furthermore, we conclude that the recombination and motility defects in the *minJ* mutant were subordinate to the impaired cell division phenotype resulting from uncontrolled MinC and MinD.

MinD activity is spatially constrained by its localization to the poles of the cell. One way in which MinJ might antagonize MinD activity is by controlling MinD localization. To monitor MinD position in the cell, a construct in which green fluorescent protein (GFP) was fused to the N-terminus of MinD and expressed from a xylose-inducible promoter (P_{xyl}) was integrated into the chromosome at the ectopic *amyE* locus (*amyE::*P_{xyl}*–GFP–minD*). To circumvent the problem that *minJ* mutants rarely form septa, a *minC* mutation was included in the parental background to increase septum frequency. Consistent with previous reports, MinD localized to cell poles in the *minC* mutant (Fig. 4C, Marston and Errington, 1999). In the *minC minJ* double mutant, however, MinD was not enriched at the cell poles but rather formed randomly distributed, membrane-associated puncta (Fig. 4D). Thus, MinJ is required for the polar localization of MinD. We speculate that the puncta of GFP–MinD observed in the *minJ* mutant might be the result of MinD self-interaction and spontaneous aggregation (see below).

MinJ might restrict MinD to the cell poles by direct protein–protein interaction. To determine protein interactions, the full-length MinC, MinD and MinJ proteins were fused to separate halves of the adenylate cyclase protein and expressed in *E. coli*. When two fusion proteins interact, they bring the two complementary halves of adenylate cyclase together, resulting in cAMP synthesis and expression of β-galactosidase from a cAMP-dependent promoter (Karimova *et al*., 1998). Thus a positive protein–protein interaction manifests as blue colonies when cells are plated on medium containing the β-galactosidase chromogenic substrate 5-bromo-4-chloro-3-indolyl β-D-galactopyranoside (X-gal). The combinations of MinC/MinC, MinD/MinD and MinJ/MinJ all gave positive results suggesting that the each protein interacted with itself (Fig. 5). Positive results were also obtained when MinD was combined with either MinC or MinJ suggesting that MinD directly interacted with both proteins (Fig. 5). The combination of MinC and MinJ did not produce a positive result suggesting that the two proteins did not directly interact. We conclude that MinJ restricts MinD to the cell poles through direct protein–protein interaction which indirectly recruits MinC.

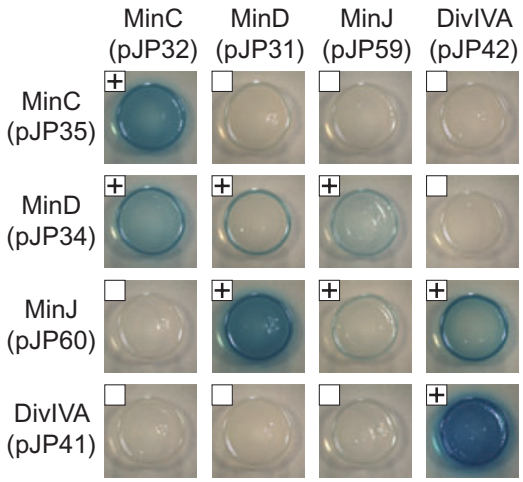

Fig. 5. MinJ interacts directly with MinD and DivIVA. A grid of colonies of *E. coli* cells is shown expressing the indicated crosses of adenylate cyclase protein fusion plasmids as indicated at the top of each column and at the edge of each row (plasmids listed in Table S1). A blue colour indicates a positive interaction between the proteins fused to adenylate cyclase whereas a white colour indicates no interaction between the proteins. Pluses in the upper left hand corner indicate that the colony was interpreted to represent a positive protein interaction whereas an open box indicates that the colony was interpreted to represent no protein interaction.

MinJ localizes after cell division has been initiated

Armed with the knowledge that FtsZ ring formation was the primary defect in *minJ* mutants and that MinJ interacted with the septal positioning machinery, we next determined the spatial and temporal localization of MinJ within the cell relative to ZapA (FtsZ rings). A strain was doubly labelled such that YFP was fused to the C-terminus of MinJ and cyan fluorescent protein (CFP) was fused to the C-terminus of ZapA and both constructs were expressed at their native loci. MinJ localized to cell

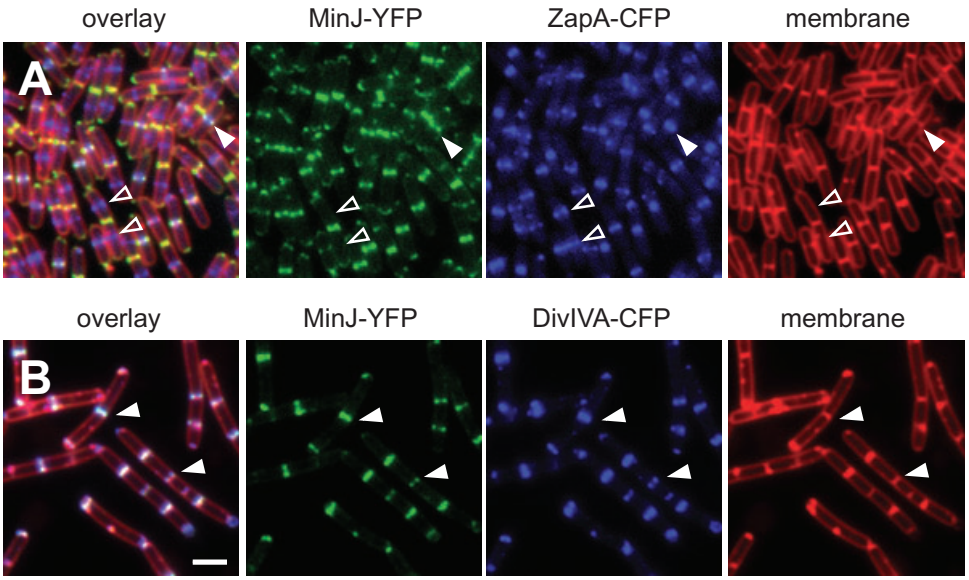

Fig. 6. Localization of MinJ relative to DivIVA and FtsZ.
A. Fluorescence microscopy of DS4075 cells expressing YFP fused to MinJ (MinJ–YFP, false coloured green) and CFP fused to ZapA (ZapA–CFP, false coloured blue) grown to exponential phase and stained with FM 4-64 (membrane, false coloured red). Open carets indicate nascent division sites at which ZapA localizes in the absence of MinJ. Closed carets indicate a site of septum formation in which MinJ puncta flank an intense ZapA focus.
B. Fluorescence microscopy of DS4154 cells expressing YFP fused to MinJ (MinJ–YFP, false coloured green) and CFP fused to DivIVA (DivIVA–CFP, false coloured blue) grown to exponential phase and stained with FM 4-64 (membrane, false coloured red). Closed carets indicate representative sites of colocalization between MinJ and DivIVA.
Scale bar is 2 μm.

poles and three patterns of localization were observed with respect to ZapA and MinJ in fluorescence micrographs (Fig. 6A). First, ZapA bands were observed prior to septum formation and these bands were not associated with MinJ (open carets, Fig. 6A). Second, MinJ and ZapA colocalized at sites of nascent septa (as indicated by membrane staining), and in these cases, dots of MinJ appeared to flank the ZapA focus (closed caret, Fig. 6A). Third, MinJ localized in the absence of ZapA at sites at which septation had been completed. Thus, ZapA localized first to nascent cell division sites, next MinJ was recruited as the septum was forming, and finally MinJ persisted at the septum after ZapA had disassociated and MinJ remained at the cell poles. We conclude that MinJ is a polarly localized topological determinant that antagonizes MinC/MinD to direct FtsZ polymerization to the midcell and also prevent re-initiation of cell division at nascent septa.

MinJ interacts with DivIVA

The phenotype of cells disrupted for MinJ was similar to that of cells disrupted for the protein DivIVA. Mutation of either *minJ* or *divIVA* gives rise to filamentous cells that can be compensated for by mutation of *minD* (Fig. 4; Edwards and Errington, 1997). Furthermore, like MinJ, DivIVA is required for MinD polar localization and DivIVA has been demonstrated to preferentially localize to old cell poles and new division septa (Edwards and Errington, 1997). To explore the relative localization of MinJ and DivIVA, a strain was doubly labelled in which yellow fluorescent protein (YFP) was fused to the C-terminus of MinJ and CFP was fused to the C-terminus of DivIVA and both constructs were expressed at their native loci. The DivIVA–CFP fusion was near fully functional. Unlike a *divIVA* null mutation, DivIVA–CFP-expressing cells were not filamentous but minicells were occasionally observed indicating a partial defect in cell division site selection (Fig. 6B). Nonetheless, DivIVA–CFP localized as bands at cell poles and division septa as reported previously, and bands of MinJ overlapped with bands of DivIVA (closed caret, Fig. 6B). Thus, MinJ and DivIVA colocalized.

To determine how the functions of MinJ and DivIVA were related, we monitored the dependence of one protein on the other for subcellular localization. Cells mutated for *minJ* rarely formed septa which might complicate the analysis of DivIVA septal localization. To mitigate this problem, a *minD* mutation was introduced to the *minJ* mutant to increase septum frequency. Consistent with previous reports, DivIVA–CFP was enriched at nascent septa and in the minicells of a *minD* single mutant (Fig. 4E; Marston *et al.*, 1998). A similar DivIVA–CFP localization pattern was observed in the *minD minJ*

double mutant (Fig. 4F). Thus, DivIVA polar localization did not depend on either MinD or MinJ.

To test the role of *divIVA* on MinJ–YFP localization, a *minD* mutation was once again included to increase septum frequency. MinJ–YFP localized to the cell poles in a *minD* single mutant (Fig. 4G). In contrast, MinJ–YFP localized to all membranes non-specifically in the *minD divIVA* double mutant (Fig. 4H). We conclude that the polar localization of MinJ requires DivIVA but not MinD. We further conclude that MinJ and DivIVA function in the same pathway to antagonize the cell division inhibitors MinC and MinD.

DivIVA might restrict MinJ to the cell poles by direct protein–protein interaction. To determine whether the MinJ and DivIVA proteins interacted, the full-length DivIVA protein was separately fused to two halves of the gene encoding adenylate cyclase, cloned into *E. coli*, and tested in the bacterial two-hybrid assay. The DivIVA/DivIVA combination gave a positive result but positive results were not obtained when DivIVA was combined with either MinC or MinD (Fig. 5). We conclude that consistent with previous reports, DivIVA interacted with itself but not with either of the cell division inhibitors. Furthermore, a positive result was obtained with only one combination of DivIVA and MinJ but nonetheless indicated an interaction between the two proteins (Fig. 5). Combined with the requirement of DivIVA for MinJ localization, the positive bacterial two-hybrid result between DivIVA and MinJ supports a model in which the two proteins directly interact. We conclude that MinJ acts as an intermediary between MinD and DivIVA to complete the polar-piloting model of cell division site selection in *B. subtilis*.

Discussion

We have identified MinJ, a new component of the Min system for cell division site placement in *B. subtilis*. Cells mutated for *minJ* grew as long filaments in which cell division septa were rare due to the inability to properly form FtsZ rings. Mutation of either *minC* or *minD* was sufficient to increase cell division in the *minJ* mutant background and therefore the normal function of MinJ is to antagonize the MinC/MinD cell division inhibitors. Thus, MinJ is genetically upstream of MinD and MinC.

The phenotype of a *minJ* mutant strongly resembled that of cells mutated for the gene encoding the topological determinant protein DivIVA (Edwards and Errington, 1997). DivIVA localizes to newly formed septa and old cell poles and sequesters MinD to those sites (Edwards and Errington, 1997; Marston *et al*., 1998). Consequently, MinD and MinC are maintained at high concentration at the poles and direct FtsZ polymerization to the midcell. MinJ acted in the same pathway as DivIVA not only because the mutant phenotypes for the two proteins were similar but also because MinJ colocalized with DivIVA in a DivIVA-dependent manner. In contrast, DivIVA localization was independent of MinJ. Thus, MinJ is cytologically downstream of DivIVA.

DivIVA is known to restrict MinD localization but no direct interaction between DivIVA and MinD has been detected. The combined genetic and cytological evidence supports a model in which MinJ acts as a bridge between MinD and DivIVA to control cell division site selection in *B. subtilis*. Consistent with this hypothesis, MinJ interacts directly with both MinD and DivIVA in a bacterial two-hybrid assay. Different domains of MinJ may interact with each protein separately. The N-terminus of MinJ is predicted to encode six consecutive transmembrane segments whereas the C-terminus of MinJ is predicted to encode a putative PDZ domain (Fig. S3). MinD is recruited to the membrane by an amphipathic alpha helix and perhaps the integral membrane domain of MinJ interacts with the membrane-anchoring domain of MinD (Hu and Lutkenhaus, 2003; Szeto *et al*., 2003). PDZ domains mediate protein–protein interactions and have been implicated in assembling multiprotein complexes (Hung and Sheng, 2002). We speculate that the PDZ domain might be the site of DivIVA interaction (Fig. S4). Alternatively, DivIVA might interact with the MinJ transmembrane domain and MinD might interact with the MinJ PDZ domain. In either scenario, the two halves of MinJ could interact with MinD and DivIVA, respectively, to sequester membrane-bound MinD to the poles of the cell.

In addition to conferring a cell division defect, mutation of *minJ* also resulted in a severe defect in homologous recombination. DNA could not be transduced and recombined into the *minJ* mutant chromosome unless the DNA being integrated encoded a complementing copy of the *minJ* gene itself. Consistent with a recombination defect, *minJ* mutants also exhibited an enhanced sensitivity to DNA damage by UV light. The requirement of MinJ for homologous recombination appeared to be indirect because a *divIVA* mutant had a similar defect in recombination and recombination could be restored to *minJ* by mutation of *minD* (Table 1). Thus, it appears that unrestricted MinD and/or MinC results in the inhibition of recombination. The inhibition of recombination by the Min system has not been reported before and may be a consequence of the undomesticated *B. subtilis* 3610 strain background. The mechanism by which Min inhibits recombination is unknown but appears to act downstream of the recombination protein RecA as RecA protein levels were similar in the wild type and the *minJ* mutant (Fig. S5). We further note that mutation of *minD* resulted in enhanced sensitivity to UV light supporting a connection of MinD to DNA repair (Fig. S1).

The *minJ* gene was reported to be essential in a laboratory strain (Calvio *et al*., 2005). Here we demonstrate

that *minJ* is non-essential in an undomesticated strain. The discrepancy over *minJ* essentiality is unlikely to be related to strain differences as we have also found that *minJ* is non-essential in the laboratory strain PY79 (data not shown). MinJ was originally deemed essential for two reasons: it was difficult or impossible to generate a *minJ* mutant, and when *minJ* was placed under an inducible promoter, the cells reportedly lysed when the inducer was depleted. The inability to generate a mutant construct may have been due to the recombination defect of *minJ* mutants and a failure to obtain colonies from certain crosses might have been interpreted as a lethal phenotype. The depletion experiment appears to have been designed such that the inducible *minJ* gene lacked the predicted *minJ* ribosome binding site (Calvio *et al*., 2005). Thus it is unclear how the protein was expressed whether or not the inducer was present. While the reason that previous results supported *minJ* essentiality are unknown, our results conclusively demonstrate that deletion of *minJ* resulted in cell filamentation and a reduction in colony-forming units but that *minJ* was otherwise dispensable for growth. In support of our results, we note that *minJ* (*yvjD*) does not appear on a published list of essential *B. subtilis* genes (Kobayashi *et al*., 2003).

We initiated our investigation into MinJ to study its role in swarming motility. The *minJ* gene was reportedly co-transcribed in an operon with the swarming motility gene *swrA*, and the two protein products were proposed to interact to regulate flagellar biosynthesis (Calvio *et al*., 2005). While it appears that *minJ* is partially co-transcribed with *swrA*, our data suggest that *minJ* is expressed from a separate promoter and that *swrA* and *minJ* do not form an obligate operon. Furthermore, the two genes appear to be phylogenetically unrelated as the *swrA* gene is found in only a limited subset of closely related *Bacillus* species whereas the *minJ* gene is conserved throughout the low G+C Gram-positive genera of *Bacillus*, *Listeria*, *Lactobacillus* and *Clostridium* (Figs S3 and S6, data not shown). In addition, we found that SwrA and MinJ are functionally unrelated because mutations that disrupt either protein impair swarming motility for different reasons. Mutation of *swrA* reduces the number of motile cells in the population and reduces the number of flagella made by the cells that are motile (Calvio *et al*., 2005; Kearns and Losick, 2005). In contrast, the swarming defect of *minJ* is not due to a decreased frequency of motility nor is it due to a defect in flagella assembly (Fig. S7). Rather, the *minJ* swarming defect is an indirect consequence of cell filamentation that constrains swarming motility into a spiralling pattern of movement (Movie S2). Furthermore, the swarming defect is not specific to *minJ* as other mutations that cause filamentation, such as *divIVA*, had a similar effect on motility and swarming was improved in both strains when cell division was increased by mutation of *minD* (Fig. 2). Cell filamentation is thought to be a prerequisite for swarming in some bacteria, and in these cases, mutations that abolish filamentation result in swarming defects (O'Rear *et al*., 1992; Belas *et al*., 1995). It seems that the opposite is true for *B. subtilis*. Wild-type *B. subtilis* cells are not filamentous during swarming motility and in fact, filamentation appears to be detrimental to surface motile behaviour.

Taken together, MinJ is a new topological determinant in *B. subtilis* that acts between DivIVA and MinD to direct FtsZ polymerization to the midcell. Mutation of *minJ* resulted in mislocalized MinD and unrestricted MinD activity had pleiotropic effects on cell physiology. MinJ is highly conserved in the low G+C group of Gram-positive bacteria and MinJ seems likely to be an important component of cell division site selection in these organisms.

Experimental procedures

Strains and growth conditions

Bacillus subtilis strains were grown in Luria–Bertani (LB) (10 g of tryptone, 5 g of yeast extract, 5 g of NaCl per litre) broth or on LB plates supplemented with 1.5% Bacto agar at 37°C. Growth was measured in a spectrophotometer reading optical density at 600 nm (OD_{600}) or by dilution plating on to LB plates. When appropriate, antibiotics were included at the following concentrations: 10 μg ml^{-1} tetracycline, 100 μg ml^{-1} spectinomycin, 5 μg ml^{-1} chloramphenicol, 5 μg ml^{-1} kanamycin, and 1 μg ml^{-1} erythromycin plus 25 μg ml^{-1} lincomycin (*mls*). Isopropyl β-D-thiogalactopyranoside (IPTG, Sigma) and X-gal (Sigma) was added to the medium at the indicated concentration when appropriate.

For the motility assay, swarm agar plates containing 25 ml of LB fortified with 0.7% Bacto agar were prepared fresh and the following day were dried for 30 min in a laminar flow hood. Each plate was toothpick inoculated from an overnight colony and scored for motility after 18 h incubation at 37°C (Kearns and Losick, 2003). Plates were visualized with a Bio-Rad Geldoc system and digitally captured using Bio-Rad Quantity One software.

β-Galactosidase assay

One millilitre of cells were harvested from a mid-log-phase (OD_{600} ~ 0.5) culture grown in LB broth shaken at 37°C, harvested and re-suspended in an equal volume of Z buffer (40 mM NaH_2PO_4, 60 mM Na_2HPO_4, 1 mM $MgSO_4$, 10 mM KCl and 38 mM β-mercaptoethanol). To each sample, lysozyme was added to a final concentration of 0.2 mg ml^{-1} and incubated at 30°C for 15 min. Each sample was diluted appropriately to 500 μl in Z buffer and the reaction was started with 100 μl of 4 mg ml^{-1} 2-nitrophenyl β-D-galactopyranoside (in Z buffer) and stopped with 250 μl of 1 M Na_2CO_3. The OD_{420} of the reaction mixtures was recorded and the β-galactosidase-specific activity was calculated according to the equation: $[OD_{420}/(\text{time} \times OD_{600})] \times$ dilution factor $\times$ 1000.

Table 2. Strains.[a]

Strain	Genotype	Reference
3610	Wild type	
DS791	*amyE::P$_{flache}$-lacZ cat*	Kearns and Losick (2005)
DS796	*amyE::P$_{swrA}$-lacZ cat*	Kearns and Losick (2005)
DS1576	*amyE::P$_{minJ}$-lacZ cat*	
DS2794	*amyE::P$_{minJ}$-minJ cat*	
DS2845	*ΔminJ amyE::P$_{hag}$-hag^{T209C}spec*	
DS2847	*ΔminJ amyE::spec*	
DS2945	*ΔminJ amyE::P$_{minJ}$-minJ cat*	
DS3185	*ΔminJ amyE::P$_{hag}$-hag^{T209C}spec minC::TnYLB* (TATATTGTTC)[b]	
DS3186	*ΔminJ amyE::P$_{hag}$-hag^{T209C}spec minD::TnYLB* (TATTGTTCA)	
DS3187	*ΔminJ amyE::P$_{hag}$-hag^{T209C}spec minD::TnYLB* (TAAATAGAG)	
DS3277	*ΔminJ amyE::kan hag::Tn10 spec*	
DS3293	*ΔminJ amyE::spec minD::TnYLB kan*	
DS3406	*ΔminJ amyE::kan srfAC::Tn10 spec*	
DS3508	*ΔminJ amyE::P$_{hag}$-hag^{T209C}spec minC::TnYLB* (TATTGCTGCT)	
DS3536	*ΔminJ amyE::P$_{hag}$-hag^{T209C}spec minC::TnYLB* (TAAAAAGCG)	
DS3537	*ΔminJ amyE::P$_{hag}$-hag^{T209C}spec minC::TnYLB* (TATTGCTGCT)	
DS3538	*ΔminJ amyE::P$_{hag}$-hag^{T209C}spec minC::TnYLB* (TATCTAAAT)	
DS3621	*zapAΩlinker–YFP spec*	
DS3774	*minD::TnYLB kan*	
DS3799	*ΔminJ zapAΩlinker–YFP spec amyE::kan*	
DS3840	*minJΩlinker–YFP spec minD::TnYLB kan*	
DS3922	*recAΩGFP spec*	
DS3941	*ΔyvD recAΩGFP spec amyE::kan*	
DS4075	*minJΩlinker–YFP spec zapAΩlinker–CFP cat*	
DS4146	*divIVA::tet*	
DS4151	*minJΩlinker–YFP spec divIVA::tet minD::TnYLB kan*	
DS4153	*divIVAΩlinker–CFP cat minD::TnYLB kan ΔminJ amyE::spec*	
DS4154	*minJΩlinker–YFP spec divIVAΩlinker–CFP cat*	
DS4155	*divIVAΩlinker–CFP cat minD::TnYLB kan*	
DS4291	*amyE::lacZ cat*	
DS4322	*minC::TnYLB kan amyE::Pxyl–GFP–minD cat*	
DS4323	*minC::TnYLB kan ΔminJ amyE::Pxyl–GFP–minD cat*	

a. All strains are in the wild-type 3610 background.
b. Sequences in parentheses indicate the site of the *mariner* transposon insertion beginning with the duplicated TA target site.

Microscopy

Fluorescence microscopy was performed with a Nikon 80i microscope with a phase-contrast objective Nikon Plan Apo 100× and an Excite 120 metal halide lamp. FM4-64 was visualized with a C-FL HYQ Texas Red Filter Cube (excitation filter 532–587 nm, barrier filter > 590 nm). CFP fluorescent signals were viewed using a C-FL HYQ CFP Filter Cube (excitation filter 426–446 nm, barrier filter 460–500 nm). YFP was visualized using a C-FL HYQ YFP Filter Cube (excitation filter 490–510 nm, barrier filter 520–550 nm). DAPI was visualized using a UV-2E/C DAPI Filter Cube (excitation filter 340–380 nm, barrier filter 435–485 nm). GFP was visualized using a C-FL HYQ FITC Filter Cube (FITC, excitation filter 460–500 nm, barrier filter 515–550 nm). Images were captured with a Photometrics Coolsnap HQ2 camera in black and white, false coloured and superimposed using Metamorph image software.

For CFP, YFP and GFP microscopy, cells were grown overnight at 22°C in LB, culture was diluted 1:100 into fresh media and grown at 22°C to OD_{600} 0.6–1.0, and 1 ml was washed once in T-Base buffer [15 mM $(NH_4)_2SO_4$, 80 mM K_2HPO_4, 44 mM KH_2PO_4, 3.4 mM sodium citrate and 3.0 mM $MgSO_4{\cdot}6H_2O$], pelleted, and re-suspended in 50 μl of T-Base buffer containing 5 μg ml^{-1} FM 4-64 and incubated for 10 min at room temperature. When appropriate, 1 μg ml^{-1} DAPI was added to the final re-suspension in T-Base buffer. Samples were observed by spotting 3 μl of suspension on a depression slide containing an agarose pad and immobilized with a poly-L-lysine-treated glass coverslip. Agarose pads were created by making a 1% solution of agarose (Fisher Brand Electrophoresis Grade) in T-Base buffer, and applying 400 μl of the molten solution to a depression slide and covering with a glass microscope slide and allowing to cool for 20 min prior to use. Images were captured with Metamorph software.

Strain construction

All constructs were first introduced into the domesticated strain PY79 by natural competence and then transferred to the 3610 background using SPP1-mediated generalized phage transduction (Yasbin and Young, 1974). All strains used in this study are listed in Table 2. All plasmids used in this study are listed in Table S1. All primers used in this study are listed in Table S2.

ΔdivIVA::tet. The *ΔdivIVA::tet* insertion deletion allele was generated by long flanking homology PCR (using primers 1305 and 1306, 1307 and 1308), and DNA containing a

tetracycline drug resistance gene (pDG1515) was used as a template for marker replacement (Guérout-Fleury *et al.*, 1995; Wach, 1996).

In-frame deletions. To generate the Δ*minJ* in-frame markerless deletion construct, the region upstream of *minJ* was PCR amplified using the primer pair 842/843 and digested with EcoRI and BamHI, and the region downstream of *minJ* was PCR amplified using the primer pair 844/845 and digested with BamHI and SalI. The two fragments were then simultaneously ligated into the EcoRI and SalI sites of pMiniMAD which carries a temperature-sensitive origin of replication and an erythromycin resistance cassette to generate pJP11. The plasmid pJP11 was introduced to PY79 by single-cross-over integration by transformation at the restrictive temperature for plasmid replication (37°C) using *mls* resistance as a selection. The integrated plasmid was then transduced into DS2794. To evict the plasmid, the strain was incubated in 3 ml of LB broth at a permissive temperature for plasmid replication (22°C) for 14 h, diluted 30-fold in fresh LB broth and incubated at 22°C for another 8 h. Dilution and outgrowth were repeated two more times. Cells were then serially diluted and plated on LB agar at 37°C. Individual colonies were patched on LB plates and LB plates containing *mls* to identify *mls*-sensitive colonies that had evicted the plasmid. Chromosomal DNA from colonies that had excised the plasmid was purified and screened by PCR using primers 842/845 to determine which isolate had retained the Δ*minJ* allele. The complementing *minJ* fragment at *amyE* was replaced by SPP1 phage transduction to generate DS2845 and DS2847.

Complementation constructs. To generate the P_{minJ}-*minJ* complementation construct (pJP17), a PCR product containing the *minJ* coding region plus 393 base pairs of upstream sequence was amplified from *B. subtilis* 3610 chromosomal DNA using the primer pair 572/983, digested with BamHI and EcoRI and cloned into the BamHI and EcoRI sites of pDG364 containing a polylinker and chloramphenicol resistance cassette between two arms of the *amyE* (Guérout-Fleury *et al.*, 1996).

GFP–MinD translational fusion. The xylose inducible *amyE::*P_{xyl}*–GFP–minD* construct was the generous gift of Dr Fredy Gueiros-Filho (Universidade de São Paulo).

MinJ–YFP translational fusion. To generate the translational fusion of MinJ to YFP, a fragment containing the terminal 600 base pairs of *minJ* coding region was amplified using 3610 as a template and primer pair 1115/1116 and was digested with SphI and XhoI and ligated into the SphI and XhoI sites of pKL183 containing a spectinomycin resistance cassette to generate plasmid pJP20 (Lemon and Grossman, 2000). A flexible linker domain was incorporated between MinJ and YFP in the fusion protein (Waldo *et al.*, 1999). The plasmid was integrated into PY79 at the native site for *minJ* by single-cross-over homologous recombination and transduced to other recipients.

ZapA–CFP and ZapA–YFP translational fusions. To generate the translational fusions of ZapA to CFP or YFP, a fragment containing the coding region of *zapA* and 288 base pairs of upstream DNA was amplified using 3610 as a template and primer pair 1117/1118 and was digested with EcoRI and XhoI and ligated into the EcoRI and XhoI sites of pKM135 containing a chloramphenicol resistance cassette or pKL183 containing a spectinomycin resistance cassette to generate plasmids pJP40 and pJP21 respectively. A flexible linker domain was incorporated between ZapA and CFP or YFP in the fusion protein. Each plasmid was integrated into PY79 at the native site for *zapA* by single-cross-over homologous recombination and transduced to other recipients. pKM135 was the generous gift from Kathy Marquis and David Rudner (Harvard Medical School).

DivIVA–CFP translational fusion. To generate the translational fusion of DivIVA to CFP, a 491-base-pair fragment containing the coding region of *divIVA* was amplified using 3610 as a template and primer pair 1301/1302 and was digested with MfeI and XhoI and ligated into the EcoRI and XhoI sites of pKM135 containing a chloramphenicol resistance cassette to generate plasmid, pJP43. A flexible linker domain was incorporated between DivIVA and CFP in the fusion protein. The plasmid was integrated into PY79 at the native site for *divIVA* by single-cross-over homologous recombination and transduced to other recipients.

Bacterial two-hybrid plasmid construction. The *minD* coding region as amplified by PCR using primer pair 1239/1240, digested with BamHI and EcoRI and ligated into the BamHI and EcoRI sites of pKT25 and pUT18C to generate plasmids pJP31 and pJP34 respectively. Similarly, the *minC* coding region was PCR amplified using primer pair 1241/1242, digested with BamHI and EcoRI, and ligated into the BamHI and EcoRI sites of pKT25 and pUT18C to generate plasmids pJP32 and pJP35 respectively. The *divIVA* coding region was PCR amplified using primer pair 1303/1304, digested with BamHI and MfeI, and ligated into the BamHI and EcoRI sites of pUT18 and pKNT25 to generate plasmids pJP41 and pJP42 and respectively. The full-length *minJ* coding region was PCR amplified using primer pair 1245/1355, digested with BamHI and EcoRI, and ligated into pUT18 and pKNT25 to generate pJP59 and pJP60 respectively. To aid in domain folding and separation, a flexible linker domain was introduced between the adenylate cyclase domain and the protein of interest by including the necessary nucleic acids in either the forward or reverse primer.

SPP1 phage transduction

To 0.2 ml of dense culture grown in TY broth (LB broth supplemented after autoclaving with 10 mM $MgSO_4$ and 100 μM $MnSO_4$), serial dilutions of SPP1 phage stock were added and statically incubated for 15 min at 37°C. To each mixture, 3 ml of TYSA (molten TY supplemented with 0.5% agar) was added, poured atop fresh TY plates and incubated at 37°C overnight. Top agar from the plate containing near confluent plaques was harvested by scraping into a 50 ml conical tube, vortexed and centrifuged at 5000 *g* for 10 min. The supernatant was treated with 25 μg ml^{-1} DNase final concentration before being passed through a 0.45 μm syringe filter and stored at 4°C.

Recipient cells were grown to stationary phase in 2 ml of TY broth at 37°C. Cells (0.9 ml) were mixed with 5 μl of SPP1 donor phage stock. Nine millilitres of TY broth was added to the mixture and allowed to stand at 37°C for 30 min. The transduction mixture was then centrifuged at 5000 *g* for 10 min, the supernatant was discarded and the pellet was re-suspended in the remaining volume. One hundred microlitres of cell suspension was then plated on TY fortified with 1.5% agar, the appropriate antibiotic, and 10 mM sodium citrate.

Transposon mutagenesis

To generate bypass mutants of Δ*minJ*, the pMarA plasmid was introduced into strain DS2845 by SPP1 phage transduction (Le Breton *et al*., 2006). Mutagenesis was performed on each isolate by growing cells in 2 ml of LB broth supplemented with kanamycin at 22°C for 24 h. Cells were diluted serially to 10^{-1}, 10^{-2} and 10^{-3}, and 100 μl of each dilution was plated on pre-warmed LB plates fortified with 1.5% agar and supplemented with kanamycin and grown at the non-permissive temperature (42°C) overnight. Colonies were pooled into 2 ml of LB broth, pelleted and re-suspended to 10 OD_{600} in 1× PBS buffer (137 mM NaCl, 2.7 mM KCl, 10 mM Na_2HPO_4 and 2 mM KH_2PO_4). Ten microlitres of the re-suspension was inoculated onto the centre of LB agar plates fortified with 0.7% agar and incubated at 37°C overnight. After overnight incubation, cells were clonally isolated from motile flares that emerged from the central colony. To confirm that the transposon was linked to the suppressor mutation, a lysate was generated on the suppressor mutant and the transposon was transduced to the parent strain lacking the suppressor. Transposon insertion sites were identified by partially degenerate touchdown PCR using primer 766 and hybrid degenerate primer 749, 50 ng of purified chromosomal DNA, and Phusion polymerase (New England Biolabs) (Levano-Garcia *et al*., 2005).

Bacterial two-hybrid assay

Bacterial two-hybrid assays were performed as described (Karimova *et al*., 1998; Van den Ent *et al*., 2006). One microlitre of each plasmid was added to 50 μl of frozen chemically competent DHM1 cells and incubated at 4°C for 30 min. Cells were heat shocked at 42°C for 90 s. One hundred and eighty microlitres of 2× YT supplemented with 20 mM glucose was added to the tubes and cells were incubated at 30°C for 45 min to recover. One hundreds microlitres of cells were spread onto LB plates supplemented with kanamycin (25 μg ml^{-1}) and ampicillin (100 μg ml^{-1}) and incubated at 30°C overnight. Single-colony transformants were inoculated into 2 ml of LB supplemented with kanamycin and ampicillin and incubated at 37°C. Ten microlitres of 1.6 OD_{600} culture was spot inoculated onto A+B minimal media plates (3.6 μM $FeCl_2{\cdot}6H_2O$, 40 μM $MgCl_2{\cdot}6H_2O$, 0.1 mM $MnCl_2{\cdot}4H_2O$, 10 mM NH_4Cl, 75 μM Na_2SO_4, 0.5 mM KH_2PO_4, 1.2 mM NH_4NO_3 and 1.5% agar) supplemented with 1 mM $MgSO_4$, 0.8% glucose, 0.0001% thiamine, 0.2% casine hydrolysate, 0.008% X-gal, 1 mM IPTG, 100 μg ml^{-1} ampicillin and 25 μg ml^{-1} kanamycin and incubated for 18 h at 30°C. Images were taken with a Leica EZ4D dissecting scope.

Acknowledgements

We thank Imrich Barák, Sigal Ben Yehuda, Jim Bever, Fredy Gueiros-Filho, Rich Losick, Lyle Simmons, Kathy Marquis, David Rudner and Graham Walker for reagents, constructs and insightful discussion. This work was supported by NSF Grant MCB-0721187 to D.B.K.

References

Belas, R., Goldman, M., and Ashliman, K. (1995) Genetic analysis of *Proteus mirabilis* mutants defective in swarmer cell elongation. *J Bacteriol* **177:** 823–828.

Bi, E., and Lutkenhaus, J. (1991) FtsZ ring structure associated with division in *Escherichia coli*. *Nature* **354:** 161–164.

de Boer, P., Crossley, R., and Rothfield, L. (1989) A division inhibitor and a topological specificity factor coded for by the minicell locus determine proper placement of the division septum in *E. coli*. *Cell* **56:** 641–649.

de Boer, P., Crossley, R., and Rothfield, L. (1992) The essential bacterial cell-division protein is a GTPase. *Nature* **359:** 254–256.

Calvio, C., Celandroni, F., Ghelardi, E., Amati, G., Salvetti, S., Ceciliani, F., *et al.* (2005) Swarming differentiation and swimming motility in *Bacillus subtilis* are controlled by *swrA*, a newly identified dicistronic operon. *J Bacteriol* **187:** 5356–5366.

Cha, J.-H., and Stewart, G.C. (1997) The *divIVA* minicell locus of *Bacillus subtilis*. *J Bacteriol* **179:** 1671–1683.

Dajkovic, A., Lan, G., Sun, S.X., Wirtz, D., and Lutkenhaus, J. (2008) MinC spatially controls bacterial cytokinesis by antagonizing the scaffolding function of FtsZ. *Curr Biol* **18:** 235–244.

Edwards, D.H., and Errington, J. (1997) The *Bacillus subtilis* DivIVA protein targets to the division septum and controls the site specificity of cell division. *Mol Microbiol* **24:** 905–915.

Edwards, D.H., Thomaides, H.B., and Errington, J. (2000) Promiscuous targeting of *Bacillus subtilis* cell division protein DivIVA to division sites in *Escherichia coli* and fission yeast. *EMBO J* **19:** 2719–2727.

Erickson, H.P. (1995) FtsZ, a prokaryotic homolog of tubulin? *Cell* **80:** 367–370.

Errington, J., Daniel, R.A., and Scheffers, D.-J. (2003) Cytokinesis in bacteria. *Microbiol Mol Biol Rev* **67:** 52–65.

Gueiros-Filho, F.J., and Losick, R. (2002) A widely conserved bacterial cell division protein that promotes assembly of the tubulin-like protein FtsZ. *Genes Dev* **16:** 2544–2556.

Guérout-Fleury, A.-M., Shazand, K., Frandsen, N., and Stragier, P. (1995) Antibiotic resistance cassettes for *Bacillus subtilis*. *Gene* **167:** 335–336.

Guérout-Fleury, A.-M., Frandsen, N., and Stragier, P. (1996) Plasmids for ectopic integration in *Bacillus subtilis*. *Gene* **180:** 57–61.

Hale, C.A., Meinhardt, H., and de Boer, P.A.J. (2001) Dynamic localization cycle of the cell division regulator MinE in *Escherichia coli*. *EMBO J* **20:** 1563–1572.

Hamoen, L.W., and Errington, J. (2003) Polar targeting of DivIVA in *Bacillus subtilis* is not directly dependent on FtsZ or PBP 2B. *J Bacteriol* **185:** 693–697.

Harry, E.J., and Lewis, P.J. (2003) Early targeting of Min proteins to the cell poles in germinated spores of *Bacillus subtilis*: evidence for division apparatus-independent recruitment of Min proteins to the division site. *Mol Microbiol* **47:** 37–48.

Howard-Flanders, P., Theriot, L., and Stedeford, J.B. (1969) Some properties of excision-defective recombination-deficient mutations of *Escherichia coli* K-12. *J Bacteriol* **97:** 1134–1141.

Hu, Z., and Lutkenhaus, J. (2003) A conserved sequence at the C-terminus of MinD is required for binding to the membrane and targeting MinC to the septum. *Mol Microbiol* **47:** 345–355.

Hu, Z., Mukherjee, A., Pichoff, S., and Lutkenhaus, J. (1999) The MinC component of the division site selection system in *Escherichia coli* interacts with FtsZ to prevent polymerization. *Proc Natl Acad Sci USA* **96:** 14819–14824.

Hu, Z., Gogol, E.P., and Lutkenhaus, J. (2002) Dynamic assembly of MinD on phospholipid vesicles regulated by ATP and MinE. *Proc Natl Acad Sci USA* **99:** 6761–6766.

Hung, A.Y., and Sheng, M. (2002) PDZ domains: structural modules for protein complex assembly. *J Biol Chem* **277:** 5699–5702.

Johnson, J.E., Lackner, L.L., and de Boer, P.A.J. (2002) Targeting of the ^{D}MinC/MinD and ^{D}MinC/DicB complexes to septal rings of *Escherichia coli* suggests a multistep mechanism for MinC-mediated destruction of nascent FtsZ rings. *J Bacteriol* **184:** 2951–2962.

Karimova, G., Pidoux, J., Ullmann, A., and Ladant, D. (1998) A bacterial two-hybrid systems based on a reconstituted signal transduction pathway. *Proc Natl Acad Sci USA* **95:** 5752–5756.

Kearns, D.B., and Losick, R. (2003) Swarming motility in undomesticated *Bacillus subtilis*. *Mol Microbiol* **49:** 581–590.

Kearns, D.B., and Losick, R. (2005) Cell population heterogeneity during growth of *Bacillus subtilis*. *Genes Dev* **19:** 3083–3094.

Kearns, D.B., Chu, F., Rudner, R., and Losick, R. (2004) Genes governing swarming in *Bacillus subtilis* and evidence for a phase variation mechanism controlling surface motility. *Mol Microbiol* **52:** 357–369.

Kobayashi, K., Ehrlich, S.D., Albertini, A., Amati, G., Andersen, K.K., Arnaud, M., *et al.* (2003) Essential *Bacillus subtilis* genes. *Proc Natl Acad Sci USA* **100:** 4678–4683.

Le Breton, Y., Mohapatra, N.P., and Haldenwang, W.G. (2006) *In vivo* random mutagenesis of *Bacillus subtilis* by use of TnYLB-1 a mariner-based transposon. *Appl Environ Microbiol* **72:** 327–333.

Lemon, K.P., and Grossman, A.D. (2000) Movement of replicating DNA through a stationary replisome. *Mol Cell* **6:** 1321–1330.

Levano-Garcia, J., Verjovski-Almeida, S., and da Silva, A.C.R. (2005) Mapping transposon insertion sties by touchdown PCR and hybrid degenerate primers. *Biotechniques* **38:** 225–229.

Levin, P.A., Margolis, P., Setlow, P., Losick, R., and Sun, D. (1992) Identification of *Bacillus subtilis* genes for septum placement and shape determination. *J Bacteriol* **174:** 6717–6728.

Levin, P.A., Shim, J.J., and Grossman, A.D. (1998) Effect of *minCD* on FtsZ ring position and polar septation in *Bacillus subtilis*. *J Bacteriol* **180:** 6048–6051.

Ma, L., King, G.F., and Rothfield, L. (2004) Positioning of the MinE binding site on the MinD surface suggests a plausible mechanism for activation of the *Escherichia coli* MinD ATPase during division site selection. *Mol Microbiol* **54:** 99–108.

Marston, A.L., and Errington, J. (1999) Selection of the midcell division site in *Bacillus subtilis* through MinD-dependent polar localization and activation of MinC. *Mol Microbiol* **33:** 84–96.

Marston, A.L., Thomaides, H.B., Edwards, D.H., Sharpe, M.E., and Errington, J. (1998) Polar localization of the MinD protein of *Bacillus subtilis* and its role in selection of the mid-cell division site. *Genes Dev* **12:** 3419–3430.

Meinhardt, H., and de Boer, P.A.J. (2001) Pattern formation in *Escherichia coli*: a model for the pole-to-pole oscillations of Min proteins and the localization of the division site. *Proc Natl Acad Sci USA* **98:** 14202–14207.

Mukherjee, A., and Lutkenhaus, J. (1994) Guanine nucleotide-dependent assembly of FtsZ into filaments. *J Bacteriol* **176:** 2754–2758.

Mukherjee, A., and Lutkenhaus, J. (1998) Dynamic assembly of FtsZ regulated by GTP hydrolysis. *EMBO J* **17:** 462–469.

Munakata, N. (1974) Ultraviolet sensitivity of *Bacillus subtilis* spores upon germination and outgrowth. *J Bacteriol* **120:** 59–65.

O'Rear, J., Alberti, L., and Harshey, R.M. (1992) Mutations that impair swarming motility in *Serratia marcescens* 274 include but are not limited to those affecting chemotaxis or flagellar function. *J Bacteriol* **174:** 6125–6137.

Osawa, M., Anderson, D.E., and Erickson, H.P. (2008) Reconstitution of contractile FtsZ rings in liposomes. *Science* **320:** 792–794.

Pichoff, S., and Lutkenhaus, J. (2005) Tethering the Z ring to the membrane through a conserved membrane targeting sequence in FtsA. *Mol Microbiol* **55:** 1722–1734.

Raskin, D.M., and de Boer, P.A.J. (1997) The MinE ring: an FtsZ-independent cell structure required for selection of the correct division site in *E. coli*. *Cell* **91:** 685–694.

Raskin, D.M., and de Boer, P.A.J. (1999) Rapid pole-to-pole oscillation of a protein required for directing division to the middle of *Escherichia coli*. *Proc Natl Acad Sci USA* **96:** 4971–4976.

Stricker, J., Maddox, P., Salmon, E.D., and Erickson, H.P. (2002) Rapid assembly dynamics of the *Escherichia coli* FtsZ-ring demonstrated by fluorescence recovery after photobleaching. *Proc Natl Acad Sci USA* **99:** 3171–3175.

Szeto, T.H., Rowland, S.L., Habrukowich, C.L., and King, G.F. (2003) The MinD membrane targeting sequence is a transplantable lipid-binding helix. *J Biol Chem* **278:** 40050–40056.

Van den Ent, F., Leaver, M., Bendezu, F., Errington, J., de Boer, P., and Löwe, J. (2006) Dimeric structure of the cell shape protein MreC and its functional implications. *Mol Microbiol* **62:** 1631–1642.

Varley, A.W., and Stewart, G.C. (1992) The *divIVB* region of the *Bacillus subtilis* chromosome encodes homologs of *Escherichia coli* septum placement (MinCD) and cell shape (MreCD) determinants. *J Bacteriol* **174:** 6729–6742.

Wach, A. (1996) PCR-synthesis of marker cassettes with long flanking homology regions for gene disruptions in *S. cerevisiae*. *Yeast* **12:** 259–265.
Waldo, G.S., Standish, B.M., Berendzen, J., and Terwilliger, T.C. (1999) Rapid protein-folding assay using green fluorescent protein. *Nat Biotechnol* **17:** 691–695.
Yasbin, R.E., and Young, F.E. (1974) Transduction in *Bacillus subtilis* by bacteriophage SPP1. *J Virol* **14:** 1343–1348.

Supporting information

Additional supporting information may be found in the online version of this article.

Please note: Wiley-Blackwell are not responsible for the content or functionality of any supporting materials supplied by the authors. Any queries (other than missing material) should be directed to the corresponding author for the article.

